

Submitted to *The Astronomical Journal*

Galaxies with a Central Minimum in Stellar Luminosity Density ¹

Tod R. Lauer

National Optical Astronomy Observatory², P.O. Box 26732, Tucson, AZ 85726

Karl Gebhardt

Department of Astronomy, University of Texas, Austin, Texas 78712

Douglas Richstone

Department of Astronomy, University of Michigan, Ann Arbor, MI 48109

Scott Tremaine

Princeton University Observatory, Peyton Hall, Princeton, NJ 08544

Ralf Bender

Universitäts-Sternwarte, Scheinerstraße 1, München 81679, Germany

Gary Bower

National Optical Astronomy Observatory, P.O. Box 26732, Tucson, AZ 85726

Alan Dressler

The Observatories of the Carnegie Institution of Washington, 813 Santa Barbara St., Pasadena, CA 91101

S. M. Faber

UCO/Lick Observatory, Board of Studies in Astronomy and Astrophysics, University of California, Santa Cruz, California 95064

Alexei V. Filippenko

Department of Astronomy, University of California, Berkeley, CA 94720-3411

Richard Green

National Optical Astronomy Observatory, P.O. Box 26732, Tucson, AZ 85726

Carl J. Grillmair

SIRTF Science Center, 770 South Wilson Avenue, Pasadena, CA 91125

Luis C. Ho

*The Observatories of the Carnegie Institution of Washington, 813 Santa Barbara St., Pasadena,
CA 91101*

John Kormendy

Department of Astronomy, University of Texas, Austin, Texas 78712

John Magorrian

Department of Physics, University of Durham, Durham, United Kingdom, DH1 3LE

Jason Pinkney

Department of Astronomy, University of Michigan, Ann Arbor, MI 48109

S. Laine, Marc Postman, & Roeland P. van der Marel

Space Telescope Science Institute, 3700 San Martin Drive, Baltimore, MD 21218

ABSTRACT

We used *Hubble Space Telescope* WFPC2 images to identify six early-type galaxies with surface-brightness profiles that *decrease* inward over a limited range of radii near their centers. The implied luminosity density profiles of these galaxies have local minima interior to their core break radii. NGC 3706 harbors a high surface brightness ring of starlight with radius ≈ 20 pc. Its central structure may be related to that in the double-nucleus galaxies M31 and NGC 4486B. NGC 4406 and NGC 6876 have nearly flat cores that on close inspection are centrally depressed. Colors for both galaxies imply that this is not due to dust absorption. The surface brightness distributions of both galaxies are consistent with stellar tori that are more diffuse than the sharply defined system in NGC 3706. The remaining three galaxies are the brightest cluster galaxies in A260, A347, and A3574. Color information is not available for these objects, but they strongly resemble NGC 4406 and NGC 6876 in their cores. The thin ring in NGC 3706 may have formed dissipatively. The five other galaxies resemble the endpoints of some simulations of the merging of two gas-free stellar systems, each harboring a massive nuclear black hole. In one version of this scenario, diffuse stellar tori are produced when stars initially bound to one black hole are tidally stripped away by the second black hole. Alternatively, some inward-decreasing surface-brightness profiles may reflect the ejection of stars from a core during the hardening of the binary black hole created during the merger.

Subject headings: galaxies: nuclei — galaxies: photometry — galaxies: structure

1. Introduction

Early-type galaxies are brightest in their centers and fade into the background at large radii. There is no shortage of parametric forms that describe this smooth progression, but all more or less presume that the density of stars reaches its maximum in the center and decreases monotonically outwards. Over the last decade, *Hubble Space Telescope (HST)* imaging has shown that galaxy centers nearly always have singular surface brightness profiles of the form $\Sigma_*(r) \sim r^{-\gamma}$ (Crane et al. 1993; Kormendy et al. 1994; Ferrarese et al. 1994; Lauer et al. 1995). Low luminosity early-type galaxies, in general, have brightness profiles that are nearly power laws over several decades in radius with $\gamma \sim 1$ into the *HST* resolution limit; for galaxies in the Virgo cluster this corresponds to radii of only a few parsecs. In contrast, the most luminous early-type galaxies have cores, defined by where the outer power law “breaks” or transitions to a shallower inner cusp — but even there, $\gamma > 0$. Lauer et al. (1995) clearly showed that even “core galaxies” had central *density* cusps, $\rho_L \propto r^{-\Gamma}$, with Γ significantly greater than zero; “power-law galaxies” typically had $\Gamma \sim 2$. Gebhardt et al. (1996) verified the Lauer et al. (1995) conclusions, showing that non-parametric inversion of the surface brightness profiles ratified the existence of density cusps in nearly all early-type galaxies imaged with *HST*.

Massive nuclear black holes may play a critical role in the origin and survival of core structure (Faber et al. 1997). This hypothesis is motivated by the dichotomy in the central structure of elliptical galaxies. The low luminosity but dense power-law galaxies will be cannibalized by the high luminosity but more diffuse core galaxies. The long-term survival of low-density cores in luminous galaxies appears to demand moderation of any mergers by the black holes; the cores should have been filled in long ago without a strong tidal field to disrupt the in-spiraling nuclei of the power-law galaxies. The theoretical work of Milosavljević & Merritt (2001) verifies the Faber et al. (1997) argument that the initial creation of a core galaxy results from the merger of two power-law galaxies, each harboring a massive nuclear black hole.

Black holes may also be required to explain the double nuclei of M31 (Lauer et al. 1993) and NGC 4486B (Lauer et al. 1996), two notable exceptions to the rule that stellar density reaches its maximum at the geometric galaxy center. The origin of these double nuclei is unknown, but their equilibrium and stability is most easily understood as a consequence of the massive black holes believed to reside in their centers (Kormendy & Bender 1999; Kormendy et al. 1997). The two visible nuclei in each galaxy are probably not distinct stellar systems, but may arise from a torus of stars bound to the black hole in a Keplerian potential (Tremaine 1995). Again, such tori may result from a merger in which two massive black holes are brought together by dynamical friction

¹Based on observations made with the NASA/ESA *Hubble Space Telescope*, obtained at the Space Telescope Science Institute, which is operated by the Association of Universities for Research in Astronomy, Inc., under NASA contract NAS 5-26555. These observations are associated with GO proposals # 5454, 5512, 6099, 6587, and 8683.

²The National Optical Astronomy Observatory is operated by AURA, Inc., under cooperative agreement with the National Science Foundation.

(Holley-Bockelmann & Richstone 2000).

In this context, we have searched for other galaxies with unusual central structures that may shed additional light on the formation of the central structure in galaxies, with particular attention to early-type systems exhibiting a central minimum in surface brightness. We identify six systems culled from a large sample of galaxies imaged by *HST* with starlight distributions that do not neatly fit into the schema that cores always have cusps with $\gamma > 0$.

2. Observations and Analysis

2.1. The Sample and Observations

The galaxies presented here were identified by searching through a heterogeneous collection of *HST* WFPC2 images of early-type galaxies. The goal was to identify systems that had minima in their stellar volume densities interior to their cores. The search criterion thus was to select galaxies that did not appear to be affected by dust absorption, but that had *projected* brightness profiles that decreased inward. This criterion is actually conservative. A core with an essentially flat profile ($\gamma \approx 0$) in projection over an extended radial range can also be consistent with an inwardly decreasing density profile. Galaxies of this sort that may bear a closer look include NGCs 1600 (Byun et al. 1996; Gebhardt et al. 1996), 4291, 5813, and 5982 (Rest et al. 2001).

Of the galaxy images examined, 51 were observed under *HST* programs GO-5512, 6099, and 6587; these are our programs to characterize the central structure of nearby early-type galaxies, with emphasis on spectroscopic searches for massive black holes. We supplemented this sample with the 15 early-type galaxies with kinematically decoupled cores observed by Carollo et al. (1997) in program GO-5454. Overall, 66 galaxies were imaged by these four programs.

Although the samples observed in each of these programs were defined with varying criteria, the observational parameters are fairly uniform. In all cases the nucleus of the galaxy was positioned at the center of the WFPC2 high-resolution PC1 chip. Images obtained in the F555W (*V*-band) filter were available for all galaxies; F814W (*I*-band) images were also available in most cases. The exposures in each filter were generally limited to a single orbit; this was usually sufficient to obtain a signal-to-noise ratio (S/N) of ~ 100 per pixel in the galaxy centers. In program GO-6587 we began to use half-pixel dither steps, allowing the construction of Nyquist-sampled images with double-sampling (Lauer 1999).

All images were deconvolved with 40 iterations of Lucy-Richardson deconvolution (Lucy 1974; Richardson 1972). This method is well-suited to WFPC2 data; Lauer et al. (1998) show examples of the deconvolution of simulated observations and compare deconvolved profiles of galaxies observed with both WFPC1 and WFPC2. The centers of the galaxies discussed in detail below were all well resolved, and the deconvolution corrections were modest. Further, in all cases, the central reductions of surface brightness were apparent in the original images; deconvolution improves the

accuracy of the photometry, but is not required to recognize the morphological features discussed below.

After we began work on this paper, an additional sample of early-type galaxies became available through the WFPC2 “snapshot” program GO-8683 (van der Marel, PI; Laine et al. 2002) on the central structure of brightest cluster galaxies (BCGs). The BCG sample consists of the Postman & Lauer (1995) set of 119 BCGs with $z < 0.05$; it is the most homogeneous set of galaxies in all five programs. These galaxies are of special interest, given the likelihood that some galactic cannibalism is still going on at this epoch, delivering faint cluster galaxies to the centers of the BCGs (Lauer 1988; Faber et al. 1997). The BCG snapshot images were only obtained with the F814W filter and PC1, and have significantly lower S/N than the more nearby galaxies. Our discussion is based on the 75 BCG images observed as of December 2001.

We discuss the six candidate galaxies with central minima in their density profiles as follows.

2.2. NGC 3706

NGC 3706 is an S0 galaxy in the Faber et al. (1989) group 242 (2749 km s⁻¹ group velocity). Its luminosity lies in the transition zone between power-law and core galaxies (Faber et al. 1997). Carollo & Danziger (1994) obtained extensive ground-based photometric and spectroscopic observations of NGC 3706; they found the galaxy to have strong central rotation and a pronounced velocity dispersion peak. The WFPC2 images show that NGC 3706 harbors a bright compact edge-on stellar ring or torus at its center (Figure 1).

A brightness profile (Figure 2) measured along the major axis of the ring shows that its surface brightness rises from the center by 0.07 mag to a local maxima at 0".13, or 21 pc from the galaxy center on both sides.³ This limb brightening suggests that the structure is not a filled disk.⁴ The image of NGC 3706 was dithered and thus has subpixels with 0".0228 scale. The profile shows the intensity at each subpixel along the major axis averaged over the width of a slice four subpixels (0".091) thick centered on the ring, with each half of the major axis averaged about the center.

A small inward decrease in surface brightness implies a larger corresponding decrease in the luminosity density profile, which is shown in Figure 3. This was computed by performing a non-parametric Abel inversion (see Gebhardt et al. 1996) of the brightness profile along the apparent ring-plane, assuming that the ring and surrounding galaxy were axisymmetric within this plane. The luminosity density of the ring has a sharply defined maximum at 0".18, or 31 pc, falling by a

³ $H_0 = 80 \text{ km s}^{-1} \text{ Mpc}^{-1}$ is adopted throughout the paper.

⁴With just one filter, it is not possible to rule out dust absorption as an alternative explanation for the central dip in the ring brightness. There is no morphological sign of dust outside the ring, however; any dust disk within the stellar disk would necessarily have a more limited radial extent and a scale height at least as compact as the stellar system.

factor of ~ 2 for $r < 0''.1$. The small increase in brightness as $r \rightarrow 0$ is of marginal significance. A rough estimate of the total ring luminosity is $\sim 1.3 \times 10^8 L_\odot$ (V -band), measured by integrating the light within a $0''.68 \times 0''.16$ slice centered on the ring, crudely corrected for the “background” galaxy light, measured in a similar slice slightly offset along the minor axis.

The thickness of the ring appears to be unresolved by *HST*. The minor-axis brightness profile (Figure 2) begins to steepen at $r < 0''.1$, which is well outside the resolution limit. However, measuring the thickness of the ring requires an assumed light distribution for the galaxy background. When simple estimates of the background are considered, it appears that the half-power point of the ring vertical extent is less than $0''.04$, or 6 pc.

The small size and extreme aspect ratio of the ring in NGC 3706 raise the issue of the ring’s lifetime against thickening by two-body relaxation. From the stellar velocity dispersion versus black-hole mass relationship of Gebhardt et al. (2000) and the velocity-dispersion observations of Carollo & Danziger (1994), NGC 3706 is expected to have a central black hole of mass $M_\bullet \approx 5 \times 10^8 M_\odot$. This mass would dominate the stellar mass enclosed within the radius of the ring and implies an angular rotation rate of $\Omega = 2.8 \times 10^{-13} \text{ s}^{-1}$ at $r = 31$ pc. If we assume a Gaussian vertical luminosity density distribution of the ring, $j(R, z) = j_0(R) \exp(-z^2/2z_0^2)$, then the upper limit on the ring thickness implies $z_0 < 5$ pc, which in turn allows calculation of an upper limit to the vertical velocity dispersion within the ring, $\sigma_z = z_0/\Omega < 43 \text{ km s}^{-1}$. If the shape of the velocity ellipsoid is similar to that in the solar neighborhood, then the isotropized dispersion is about 1.5 times as large, or $\sigma < 64 \text{ km s}^{-1}$. At the upper limit for the dispersion, the relaxation time (Binney & Tremaine 1987) within the ring is

$$t_r = 0.34\sigma^3 (G^2 m \rho \ln \Lambda)^{-1} \quad (1)$$

$$= 3 \times 10^{11} \text{ yr} \left(\frac{1M_\odot}{m} \right) \left(\frac{M}{L} \right)^{-1}, \quad (2)$$

where we have adopted a midplane density $\rho_0 = 10^3 M_\odot \text{ pc}^{-3}$ (see Figure 3), the mass-to-light ratio M/L is in solar units, the stars are assumed to have solar mass, and $\ln \Lambda = \ln(1.2z_0\sigma^2/(GM_\odot)) = 16$. This result for the relaxation time is consistent with the hypothesis that the ring age is comparable to a Hubble time. However, the dependence of t_r on σ and ρ_0 implies $t_r \propto z_0^{-4}$; thus t_r may be substantially shorter than the present estimate, and the actual ring thickness could be determined by two-body relaxation if z_0 were a factor of two or more smaller than the observational upper limit.

The brightness of the ring falls rapidly from $r \approx 0''.2$ to $r \approx 0''.4$, where an inflection point in the major axis luminosity density profile occurs. The ring is actually misaligned with the major axis of the galaxy at large radii, as can be seen in the contour map (Figure 4) and plot of isophote position angle (PA; Figure 5). The PA of the ring is 114° , as compared to the galaxy PA of 78° for isophotes with $r > 5''$. Even though the bright portion of the ring is compact, the transition of PA from the ring to outer-galaxy isophote orientation takes place smoothly over $0''.5 < r < 2''.0$; this is a strong twist, given the high ellipticity of the isophotes over the same radii.

The existence of this twist raises an interesting dynamical problem. If the isodensity surfaces in the galaxy are triaxial ellipsoids with aligned principal axes, then isophote twists can arise if the axis ratios of the isodensity surfaces vary with radius and the line of sight does not lie in one of the principal planes (e.g., Binney & Merrifield 1998). However, in NGC 3706 we see the ring edge-on. Therefore the isophote twist between $0''.5$ and $2''.0$ implies that the ring plane is not one of the principal planes of the galaxy at larger radii (> 300 pc). Thus the tidal force from the galaxy must induce precession of the ring plane; crude estimates suggest that the precession time is a few times 10^8 yr. Gravitational interactions between the precessing ring plane and passing stars from the host galaxy can damp or excite the inclination of the ring (Dubinski & Kuijken 1995; Nelson & Tremaine 1995); the damping timescale is difficult to estimate accurately but typically is only a few precession times and hence probably is short compared to a Hubble time. The non-zero inclination might then indicate either that the ring was young, or that the interactions with the host galaxy have excited the inclination of a ring that was initially located in or near the equatorial plane of the galaxy.

We stress that it is essentially impossible to decompose NGC 3706 uniquely into separate background galaxy and ring components; however, the minor-axis surface brightness profile does appear to “break” at $r \approx 0''.2$, which is outside radii associated with the ring itself. The slope of the minor axis profile for $0''.1 < r < 0''.2$ is $\gamma \approx 0.4$, suggestive of a transition to a shallow cusp. NGC 3706 thus appears to be a core galaxy.

2.3. NGC 4406

NGC 4406 is a giant elliptical galaxy in the Virgo cluster. NGC 4406 rotates slowly about its *major* axis (Wagner et al. 1988; Franx et al. 1989), but its core interior to $r < 5''$ rotates rapidly about the minor axis (Bender 1988; Franx et al. 1989) and has significantly higher line-strengths compared to the envelope (Bender & Surma 1992), intriguing results in light of the following discussion. Carollo et al. (1997) obtained F555W and F814W WFPC2 images of NGC 4406 as part of their sample of elliptical galaxies with kinematically distinct cores. They found NGC 4406 to have a well-resolved core with a “break radius” $r_b = 0''.95$, with a ring of reduced surface brightness interior to this radius. Carollo et al. believed that this “moat” (our coinage) was due to dust absorption, but noted that no reddening was seen in a comparison of V and I images. We argue instead that the moat is a true reflection of the starlight distribution in NGC 4406. One possibility is that NGC 4406 began with a normal core, and that some of the stars in the region interior to the core break radius were subsequently ejected; a second is that a diffuse stellar torus is encircling the nucleus at slightly larger radii, creating the appearance of reduced surface brightness interior to the torus (this could either be a face-on torus or a thick edge-on torus; for reasons given below we prefer the latter interpretation).

Figure 6 shows the deconvolved WFPC2 F555W and F814W images of NGC 4406, as well as an STScI *HST* archive F160W NIC2 image of the same region obtained by Ravindranath et al. (2001).

A moat of reduced emission is visible in all three images. Figure 7 shows the F555W major axis and minor-axis surface brightness profiles of NGC 4406. For $r > 1''.2$, the profiles were derived by the standard fitting of ellipses to the isophotes; at smaller radii, where the isophotes were poorly fitted by ellipses, the profiles consist simply of cuts along each axis (of $0''.14$ width), with the opposite sides about the nucleus averaged. The moat of reduced emission is visible as a local minimum in the major axis brightness profile (PA= 127°) at $0''.11$ from the nucleus. The profile then brightens outward by 0.07 mag to a maximum at $0''.49$ from the nucleus. The minor-axis profile is somewhat flatter over the same radii, with the surface brightness rising only 0.02 mag outward to a maximum at $0''.38$ (29 pc) from the nucleus. Both profiles show a sharp peak at the smallest radii, which appears to be a poorly-resolved nuclear point source.

Carollo et al. (1997) noted the somewhat lower maximum brightness along the minor axis and argued that their “dust ring” was elongated in this direction. An equivalent picture, however, is that we are looking at a diffuse, edge-on, thick torus of stars that in projection is elongated along the major axis; this interpretation is made somewhat more explicit by the contour map presented in Figure 8. In this case it is natural to assume that both the background galaxy and the torus are axisymmetric with respect to the projected minor axis of the galaxy, and symmetric with respect to the plane formed by the line of sight and the projected major axis. We are motivated to consider a dustless interpretation both by the example of a stellar torus in NGC 3706, and by the lack of any dust reddening in NGC 4406. Figure 6 shows that the $V - I$ color map made by dividing the F555W by the F814W image is devoid of any structure or gradients over the extent of the core. NGC 4406 does have a red color gradient as $r \rightarrow 0$, with $\Delta(V - I)/\Delta \log(r) = -0.062$ for $1'' < r < 10''$ (Figure 9), but this color gradient is completely normal for giant elliptical galaxies (Carollo et al. 1997). The color for $r < 1''$ actually appears to be constant with $V - I = 1.31 \pm 0.01$ mag. The color of the moat, itself, measured from all pixels falling within the annulus $0''.13 < r < 0''.26$ is $V - I = 1.309 \pm 0.006$ mag, as compared to $V - I = 1.303 \pm 0.006$ mag measured in two $0''.32$ square patches centered on the points of maximum surface brightness on each side of the nucleus. From the extinction tables in Holtzman et al. (1995), we infer $A_V \approx 2.5\Delta(V - I)$ for the WFPC2 filter-set. The difference $\Delta(V - I) = 0.006 \pm 0.009$ mag is insignificant, and the implied A_V is clearly insufficient to account for the moat of reduced surface brightness.

The case against dust absorption is made particularly strong by the close similarity of the F160W NIC2 image to the WFPC2 images (information that was not available to Carollo et al. 1997). Again, the $V - H$ color (Figure 9) is essentially flat over the core interior; if anything, the $V - H$ may become slightly *bluer* interior to the radius of maximum brightness in the core.

If the unusual core of NGC 4406 reflects the intrinsic distribution of starlight, then a ring of even slightly reduced surface brightness implies a stronger corresponding decrease in luminosity density. Figure 10 shows the implied major axis luminosity density profile obtained from nonparametric Abel inversions of the profiles shown in Figure 7, again done under the assumption that the galaxy is axisymmetric in the plane defined by the major axis and line-of-sight. The 0.07 mag inward decrease in surface brightness on the major axis corresponds to a factor of 2 to 30 decrease in

luminosity density over the same radii. The exact density profile is clearly sensitive to small changes in the brightness profile; however, we note that even for a perfectly flat light profile, NGC 4406’s core is sharp enough ($\gamma = 0$ but $\alpha > 2$ in the parametric form of Lauer et al. 1995) that an inward decrease in volume density would still be implied.

It is ambiguous as to whether the NGC 4406 density profile has been created by either adding stars to or removing them from an originally normal core. Fits to the V -band profile give $I_b = 16.03$ mag arcsec $^{-2}$ and $r_b = 0''.93$, corresponding to 72 pc at an assumed distance of 16 Mpc. This implies that NGC 4406 has a normal core for its luminosity (Faber et al. 1997). There is no unique way to decompose the density profile into a torus superimposed on a more normal density profile. Under some assumptions, such an exercise could imply that NGC 4406 had a substantially larger core prior to some sort of accretion event; scatter in the $L - r_b$ and $L - I_b$ relationships is too large to rule this out (Faber et al. 1997). Conversely, NGC 4406 may have had a *smaller* core prior to the event — indeed, it is within the luminosity range of the power-law galaxies, which have no cores at all. One could thus argue that the present density profile represents an evacuation of a plausibly more concentrated initial profile.

2.4. NGC 6876

NGC 6876 is a giant elliptical galaxy in the Pavo, or Faber et al. (1989) group 269 (4078 km s $^{-1}$ group velocity). Its luminosity is typical for a core galaxy (Faber et al. 1997). Figure 11 shows the deconvolved WFPC2 F555W and F814W images of NGC 6876. The depression in surface brightness interior to the core is subtle, but is evident as a reduced band of surface brightness along the minor axis in both colors. A contour map (Figure 12) of the slightly smoothed F814W image also highlights the unusual structure. The inner isophotes of NGC 6876 become increasingly flattened, ultimately developing an indentation on the minor axis; NGC 6876 appears to have a diffuse edge-on torus of starlight added to an otherwise normal core.

Figure 13 shows the F555W major axis and minor-axis surface brightness profiles of NGC 6876. For $r > 0''.7$, the profiles were derived by the standard fitting of ellipses to the isophotes; at smaller radii, where the isophotes were poorly fitted by ellipses, the profiles consist simply of cuts along each axis (of $0''.23$ width), with the opposite sides about the nucleus averaged. The point of maximum brightness along the major axis occurs at $0''.24$ (60 pc) from the nucleus, where the surface brightness has brightened by 0.02 mag over its central value. The minor-axis profile actually has a cusp with γ slightly positive over the same radii, again suggestive of a diffuse torus that has its points of maximum projected brightness offset along the major axis. Looking to larger radii, it is noteworthy that the major axis brightness profile for $1'' < r < 3''$ has a steeper power-law index than that of the envelope at $r > 3''$. NGC 6876 thus has a subtle form of a “nuclear rise” exterior to its nominal core.

The similar appearance of NGC 6876 in both the V and I filters implies that its unusual core

morphology is not due to dust. The $V - I$ map in Figure 11 shows no structure. The average $V - I$ color in two $0''.32$ boxes (7×7 pixels) centered on the maxima of the presumed torus at $0''.31$ on either side of the center is 1.326 ± 0.005 mag, as compared to 1.328 ± 0.007 mag for the same-sized box about the center, itself; the net difference $\Delta(V - I) = 0.002 \pm 0.009$ mag going from the outer core into the center is clearly insignificant. At the same time, since $A_V \approx 2.5\Delta(V - I)$ and the central dimming is only 0.02 mag in V , it may be difficult to rule out an alternative model consisting of weak dust absorption in a core with an exceedingly weak cusp. As noted above, a uniformly flat core for $r < 0''.24$ would still imply a stellar *density* profile that decreased at smaller radii. For cusps steeper than even $\gamma \approx 0.02$, however, the implied dust absorption and associated $V - I$ reddening would already be inconsistent with the observations.

It is noteworthy that the PA of the innermost isophotes, $PA = 89^\circ$, is twisted by 13° from the major axis of the galaxy at $r > 2''.9$ ($PA = 76^\circ$); given the high ellipticity of the inner isophotes, this apparently modest twist is actually highly significant. As with NGC 3706, the isophote ellipticity and PA profiles of NGC 6876 (Figure 14) suggest that its torus is a more extensive system than might be inferred from the small radius of the major axis brightness profile maximum. The implied dip in stellar density (Figure 15) is less impressive than those in NGC 3706 and NGC 4406, but still shows a significant inward decrease.

2.5. Brightest Cluster Galaxies

A search through the *HST* “snapshot” images of BCGs discussed in §2.1 turned up a few more candidates for galaxies with dips in their core brightness profiles. As the snapshot images were only obtained in F814W and have relatively low S/N, it is more difficult to rule out dust absorption — already clearly evident in many BCGs — as an explanation for such galaxies. BCG candidates for galaxies with true local minima in their stellar density profiles were those that most closely resembled the three galaxies discussed above. That is, the minima had to be diffuse in appearance, and bracketed by bilaterally symmetric brightness maxima. The first criterion yielded 10 candidates from the sample of 72 observed so far; addition of the second criterion limited the final candidate list to three BCGs (A260, A347, and A3574). Images of the centers of the three galaxies are shown in Figure 16 and symmetrized major axis brightness traces are presented in Figure 17.

A347 is the best candidate for a BCG with a stellar torus. Its isophotes become highly flattened at small radii, and its central brightness minimum is clearly evident. A3574 and A260 have large diffuse cores that on close examination have subtle ($\sim 2\%$) surface brightness depressions along the major axes interior to their break radii. Demonstration that dust is not playing a role in all three BCGs requires deeper exposures in at least two colors.

3. Discussion

It is possible that all six galaxies identified in this paper harbor stellar tori superimposed on normal cores. Certainly, the bright and sharply defined feature in NGC 3706 is difficult to explain as anything else. It is tempting to include M31 and NGC 4486B in this class, since the Tremaine (1995) model for M31 is based on a stellar torus, even though two brightness maxima (“double nuclei”) in both galaxies are more pronounced and are less symmetric than in the galaxies described here. The origin of such tori will be discussed further below, as well as the hypothesis that some of the “tori” may really be cores that have been partially evacuated.

In either case, a genuine minimum in the density profile implies significant rotation, triaxiality, or anisotropy. An inward decrease in density cannot occur in spherical galaxies whose phase-space distribution functions depend only on the energy. Such functions are guaranteed to be solutions of the collisionless Boltzmann equation. The density in this case for a spherical system is given by

$$\rho = 2^{3/2} \pi \int_0^\psi f(\epsilon)(\psi - \epsilon)^{1/2} d\epsilon, \quad (3)$$

where $f \geq 0$ is the mass per unit volume of phase space, $\epsilon \equiv -E$, and $\psi \equiv -\Phi$ (the quantities ϵ (total energy) and ψ (gravitational potential) are defined so that we work with non-negative variables: $\psi(r)$ is positive at all radii, and ϵ is positive for all bound stars). We can use

$$d\rho/d\psi = 2^{1/2} \pi \int_0^\psi f(\epsilon)(\psi - \epsilon)^{-1/2} d\epsilon \quad (4)$$

to evaluate the density gradient anywhere in the galaxy (note that the derivative with respect to the upper limit of the integral is zero because the integrand goes to zero). Since ψ is a function only of radius, the gravitational field and any density gradient are both radial, and the latter is

$$\frac{d\rho}{dr} = \frac{d\psi}{dr} \frac{d\rho}{d\psi}. \quad (5)$$

Since $d\psi/dr = -GM(r)/r^2$ is always negative and $d\rho/d\psi$ is always positive [$f(\epsilon)$ is non-negative for all ϵ], $d\rho/dr$ is always negative in any spherical system in which the distribution function depends only on energy. Thus, the systems observed in this paper are guaranteed to be either nonspherical or anisotropic, and may be both. All the systems for which we have dynamical observations indeed appear to have significant central rotation. The rotation amplitude in NGC 4406 is modest, but it is strong in M31, NGC 3706, and NGC 4486B.

We next discuss two possibilities for the formation of the toroidal stellar systems.

3.1. Star Formation and Nuclear Disks

There are several elliptical galaxies or bulges that harbor central stellar disks. Kormendy et al. (2002) present a short list of examples and argue that these disks were created *in situ* by accreted

gas funneled into the center. Scorza & van den Bosch (1998) emphasize that the disks can be radially compact and of high surface brightness. One might then ask if the tori in the present systems result from *in situ* star formation as well. Of the six galaxies, the relatively cold and dense ring in NGC 3706 comes closest to resembling a stellar disk formed directly from a gas disk. One possible scenario is that the overall core structure was formed by the cannibalization of a low-mass stellar system, which contained some amount of gas, by NGC 3706. As is discussed in §2.2, the ring in NGC 3706 is embedded in a larger stellar system that itself rises above and is twisted from the envelope brightness profile. This system would contain the pre-existing stars in the denser portions of the cannibalized object, while the abrupt transition to the bright ring, itself, would reflect stars formed by gas delivered to the center of NGC 3706 in the same merger event. The issues remain: (1) Why has the ring not been filled in? (2) Why has the ring and surrounding stellar system not settled to the midplane defined by the envelope? Presently, the maximum ring density falls well inside the Roche radius of the estimated nuclear black hole mass. Thus, star formation in the ring requires either that the black hole was initially less massive, or that the pre-existing gas was in the form of dense molecular clouds, or that the gas layer in the disk was thinner than the current stellar disk.

The tori in the five remaining galaxies, however, appear to be considerably more diffuse and are less suggestive of thin stellar disks than the ring in NGC 3706. Further, the transition from the outer cores to the radii of the tori appears to be smooth and gradual — there is no abrupt transition to a high surface brightness ring, as is seen on the minor axis of NGC 3706. While it may be likely that these remaining tori were created in a merger event, as well (as we argue below), there is presently no compelling evidence that suggests that gas infall, followed by star formation within the cores, played a role in their formation.

3.2. Mergers of Galactic Nuclei Containing Black Holes

It is now believed that the orbital decay of the massive black holes added to a galaxy by mergers with other galaxies may largely determine the inner distribution of starlight in the merger remnant. We speculate that the unusual structures seen in the present sample (with the possible exception of NGC 3706) may be evidence of this process. As it happens, both the “stellar torus added” and “evacuated core” interpretations of the observations may be supported by this scenario.

Begelman et al. (1980) argued that galaxies harboring massive black holes should occasionally merge and sketched out the orbital decay of the binary black hole that would be created in such an event. Among other predictions, they suggested that in the later stages of the binary’s life, the two black holes would eject stars from the newly merged core as the binary hardened, creating a local minimum in stellar density at the few parsec scale. Ebisuzaki et al. (1991) studied this problem numerically and showed that the binary black hole would generate a core with a shallow cusp in the merger remnant. Intriguingly, Makino (1997) showed that local minima in stellar density occurred within the core in some simulations.

The preservation of cores during mergers essentially demands that the final stages of such events are dominated by nuclear black holes (Faber et al. 1997). The central density contrast between core and power-law galaxies is strong enough that even modest cannibalism of the latter by the former should have filled in the diffuse cores long ago. The “core within a core” merger endpoint hypothesized by Kormendy (1984) prior to *HST* observations, however, has never been found. The tidal field of the nuclear black hole solves this problem by shredding the incoming nucleus prior to its final delivery to the center. That cores exist only in the more luminous non-rotating elliptical galaxies, where gaseous dissipation may be less important during the merging of their progenitors, bolsters this picture (Faber et al. 1997).

All six galaxies discussed here appear to be core galaxies. The strong central isophote twist in NGC 3706 and the kinematically decoupled core in NGC 4406 suggests that mergers have influenced the inner structure of both galaxies. The increase in isophote ellipticity in NGC 6876 and A347 with decreasing radius, but at radii larger than at of the putative stellar tori, may also suggest cannibalization of a pre-existing stellar system. The cannibalized system would be less luminous, but denser and dynamically colder — the ellipticity increase would reflect stars from such a galaxy being preferentially deposited in the core of the more luminous galaxy.

One immediate concern is why evacuated cores are so rare if they are a natural consequence of the process (decaying binary black holes) that is supposed to make all cores. It is noteworthy that the recent simulations of Milosavljević & Merritt (2001) only produced the $\gamma > 0$ cusps seen in “normal” core galaxies. The nearly constant density cores generated by Makino (1997), let alone cores with dips in density, were not seen. Significantly, Milosavljević & Merritt (2001) always merged two power-law galaxies to test the initial formation of a core as advocated by Faber et al. (1997), while Makino (1997) started with cores already present in the merging galaxies. In a merging hierarchy, the more luminous galaxies may experience multiple episodes of merging or cannibalism. If a merger product is used as the input for subsequent mergers, then there is a variety of possible initial structural forms. Two core galaxies may merge, a core galaxy may cannibalize a power-law galaxy, and so on; allowing for the concentration of the pre-merger cores provides an additional variable. If the Milosavljević & Merritt (2001) simulations are correct for the original formation of a core galaxy, but the Makino (1997) simulations are correct that central evacuation can occur with appropriate initial conditions, then perhaps the rarity of observational examples of evacuated cores merely reflects the likelihood of these conditions.

As the black hole binary hardens, it will eject stars from the merged core to increasingly large distances. Early in its life, however, when the separation of the two black holes is similar to the core break radius, tidally stripped stars originally bound to either hole may still linger within the core. Holley-Bockelmann & Richstone (2000) emphasize that under some circumstances, such as when one galaxy has a relatively high nuclear stellar density and arrives at the center of the other galaxy with a high impact parameter, stars stripped from the incoming galaxy may form a diffuse torus. Zier & Biermann (2001) have also discussed the formation of a stellar torus as one black hole strips stars from the other. In this picture, we really are seeing diffuse stellar tori superimposed against

the cores of the merger remnants. Ironically, Holley-Bockelmann & Richstone (2000) attempted to explain the thin nuclear disks (as discussed in the context of NGC 3706) as being created by this process, but noted that they could only generate diffuse tori, not the high aspect-ratio disks seen in systems like NGC 3115 or NGC 4594. Some of the present systems may be the realizations of the toroidal structures seen in the Holley-Bockelmann & Richstone (2000) simulations.

4. Summary

We have discussed six early-type galaxies in which the luminosity density distribution in the core cannot be represented as a simple power law. The surface brightness profiles of all six systems decrease over limited radii interior to their cores. This implies that there are correspondingly more pronounced dips in their luminosity density profiles. In the systems for which we have multi-color imaging (NGC 4406 and NGC 6876), it is unlikely that we are being confused by some low level of diffuse dust absorption. The three BCG strongly resemble these two systems, and they show no compact dust clouds anywhere around their cores. We have therefore included them within this discussion, although additional multicolor imaging of the BCG should be obtained to verify this conclusion. The final system, NGC 3706, harbors a bright, apparently edge-on stellar ring.

There are two literally complementary interpretations of the core structures seen in the six galaxies. The first picture is that we are seeing stellar tori superimposed on otherwise normal cores. The narrow ring in NGC 3706 stands in such strong contrast with its surrounding core that it is difficult to accept any alternative interpretation. NGC 3706, and perhaps some of the five remaining systems, may be related to the double-nucleus galaxies M31 and NGC 4496B. The six galaxies discussed here did not present themselves as double nuclei; however, as they all do have subtle local maxima in surface brightness that bracket their apparent nuclear centers, it would take only a modest brightness enhancement at these locations to have them appear as doubles. Instead, perhaps the more suggestive presence of stellar tori in the present galaxies bolsters the plausibility of this interpretation for M31 and NGC 4486B, as well.

The thinness of the NGC 3706 torus probably requires it to have formed dissipatively. The core structure of NGC 3706 suggests that it and the inner ring were formed in a merger or cannibalism of a stellar system that contained some amount of gas. In the “torus-added” picture the tori in the remaining systems may have formed from the cannibalization of gas-free stellar systems. In this case, the tori would have been generated by the tidal disruption of the cores or central cusps of the original systems by a massive black-hole binary formed from the nuclear black holes contained in the original systems.

In the second picture we are seeing a true depletion of stars within the cores of the galaxies. As in the picture above, a black hole binary would be formed in a merger. As the binary hardens, it ejects stars from the core. The difference between this picture and the “torus-added” scenario may be one of initial conditions, in which ejection of stars at later stages in the binary’s evolution

competes against deposition of relatively colder stars around the core at an earlier stage in the binary’s life for domination of the final integrated structure of the core.

The “core-evacuated” scenario is suggested by theoretical results that are only weakly evident in some merger simulations. If core evacuation does occur, it may require rare initial conditions. The Milosavljević & Merritt (2001) simulations argue that evacuation is not likely to be seen in the merger of two power-law galaxies that would create a core galaxy initially. It may be that evacuated cores can occur in subsequent mergers in which at least one of the two galaxies already contains a core.

Regardless of which scenario is correct, we present the six galaxies as interesting probes on the formation of cores. Theoretical and observational work both point to a strong role for nuclear black holes for establishing the core structure of merger remnants. Rare and unusual core structures may offer a unique narrative in this story not otherwise voiced by more normal galaxies.

We thank Joseph Jensen for providing the reduced NIC2 images of NGC 4406. Support for GO proposals 5512, 6099, 6587, and 8683 was provided by NASA through grants from the Space Telescope Science Institute, which is operated by the Association of Universities for Research in Astronomy, Inc., under NASA contract NAS 5-26555.

Table 1. Observational Summary

Galaxy	D (Mpc)	M_B (mag)	A_B (mag)	Images
NGC 3706	35	−21.24	0.36	500 s F555W (2×2 subsampled)
NGC 4406	16	−21.26	0.11	500 s F555W, 500 s F814W, 140 s F160W
NGC 6876	51	−22.43	0.16	4100 s F555W, 4100 s F814W

Note. — $H_0 = 80 \text{ km s}^{-1} \text{ Mpc}^{-1}$ is assumed. Group velocities were used for distance estimation.

REFERENCES

- Begelman, M. C., Blandford, R. D., & Rees, M. J. 1980, *Nature*, 287, 307
- Bender, R. 1988, *A&A*, 202, L5
- Bender, R., & Surma, P. 1992, *A&A*, 258, 250
- Binney, J., & Merrifield, M. 1998, *Galactic Astronomy* (Princeton: Princeton Univ. Press) p. 183
- Binney, J., & Tremaine, S. 1987, *Galactic Dynamics* (Princeton: Princeton Univ. Press) p. 514
- Byun, Y. I., et al. 1996, *AJ*, 111, 1889
- Carollo, C. M., & Danziger, I., J. 1994, *MNRAS*, 270, 523
- Carollo, C. M., Franx, M., Illingworth, G. D., & Forbes, D. 1997, *ApJ*, 481, 710
- Crane, P., et al. 1993, *AJ*, 106, 1371
- Dubinski, J., & Kuijken, K. 1995, *MNRAS*, 283, 618
- Ebisuzaki, T., Makino, J., & Okumura, S. K. 1991, *Nature*, 354, 212
- Faber, S. M., Tremaine, S., Ajhar, E. A., Byun, Y., Dressler, A., Gebhardt, K., Grillmair, C., Kormendy, J., Lauer, T. R., & Richstone, D. 1997, *AJ*, 114, 1771
- Faber, S. M., Wegner, G., Burstein, D., Davies, R. L., Dressler, A., Lynden-Bell, D., & Terlevich, R. J., 1989, *ApJS*, 69, 763
- Ferrarese, L., van den Bosch, F. C., Ford, H. C., Jaffe, W., & O'Connell, R. W. 1994, *AJ*, 108, 1598
- Franx, M., Illingworth, G., & Heckman, T. 1989, *ApJ*, 344, 613
- Gebhardt, K., Richstone, D., Ajhar, E. A., Lauer, T. R., Byun, Y., Kormendy, J., Dressler, A., Faber, S. M., Grillmair, C., & Tremaine, S. 1996, *AJ*, 112, 105
- Gebhardt, K., et al. 2000, *ApJ*, 539, L13
- Holley-Bockelmann, K., & Richstone, D. O. 2000, *ApJ*, 531, 232
- Holtzman, J. A., Burrows, C. J., Casertano, S., Hester, J. J., Trauger, J. T., Watson, A. M., & Worthey, G. 1995, *PASP*, 107, 1065
- Kormendy, J. 1984, *ApJ*, 287, 577
- Kormendy, J., & Bender, R. 1999, *ApJ*, 522, 772
- Kormendy, J., Bender, R., Magorrian, J., Tremaine, S., Gebhardt, K., Richstone, D., Dressler, A., Faber, S. M., Grillmair, C., & Lauer, T. R. 1997, *ApJ*, 473, L91

- Kormendy, J., Dressler, A., Byun, Y.-I., Faber, S. M., Grillmair, C., Lauer, T. R., Richstone, D., & Tremaine, S. 1994, in *ESO/OHP Workshop on Dwarf Galaxies*, ed. G. Meylan and P. Prugniel (Garching: ESO), p. 147.
- Kormendy, J., Gebhardt, K., Macchetto, F. D., & Sparks, W. B. 2002, *AJ*, submitted; astro-ph/0107218
- Laine, S., Lauer, T. R., van der Marel, R. P., & Postman, M. 2002, in preparation
- Lauer, T. R. 1988, *ApJ*, 325, 49
- Lauer, T. R. 1999, *PASP*, 111, 227
- Lauer, T. R., et al. 1993, *AJ*, 106, 1436
- Lauer, T. R., Ajhar, E. A., Byun, Y.-I., Dressler, A., Faber, S. M., Grillmair, C., Kormendy, J., Richstone, D., & Tremaine, S. 1995, *AJ*, 110, 2622
- Lauer, T. R., Faber, S. M., Ajhar, E. A., Grillmair, C. J., & Scowen, P. A. 1998, *AJ*, 116, 2263
- Lauer, T. R., Tremaine, S., Ajhar, E. A., Bender, R., Dressler, A., Faber, S. M., Gebhardt, K., Grillmair, C., Kormendy, J., & Richstone, D. 1996, *ApJ*, 471, L79
- Lucy, L. B. 1974, *AJ*, 79, 745
- Makino, J. 1997, *ApJ*, 478, 58
- Milosavljević, M., & Merritt, D. 2001, *ApJ*, 563, 34
- Nelson, R. W., & Tremaine, S. 1995, *MNRAS*, 275, 897
- Postman, M., & Lauer, T. R. 1995, *ApJ*, 440, 28
- Ravindranath, S., Ho, L. C., Peng, C. Y., Filippenko, A. V., & Sargent, W. L. W. 2001, *AJ*, 122, 653
- Rest, A., van den Bosch, F. C., Jaffe, W., Tran, H., Tsvetanov, Z., Ford, H. C., Davies, J., & Schafer, J. 2001, *AJ*, 121, 2431
- Richardson, W. H. 1972, *J. Opt. Soc. A.*, 62, 52
- Scorza, C., & van den Bosch, F. C. 1998, *MNRAS*, 300, 469
- Tremaine, S. 1995, *AJ*, 110, 628
- Wagner, S. J., Bender, R., & Möllenhoff, C. 1988, *A&A*, 195, L5
- Zier, C., & Biermann, P. L. 2001, *A&A*, 377, 23

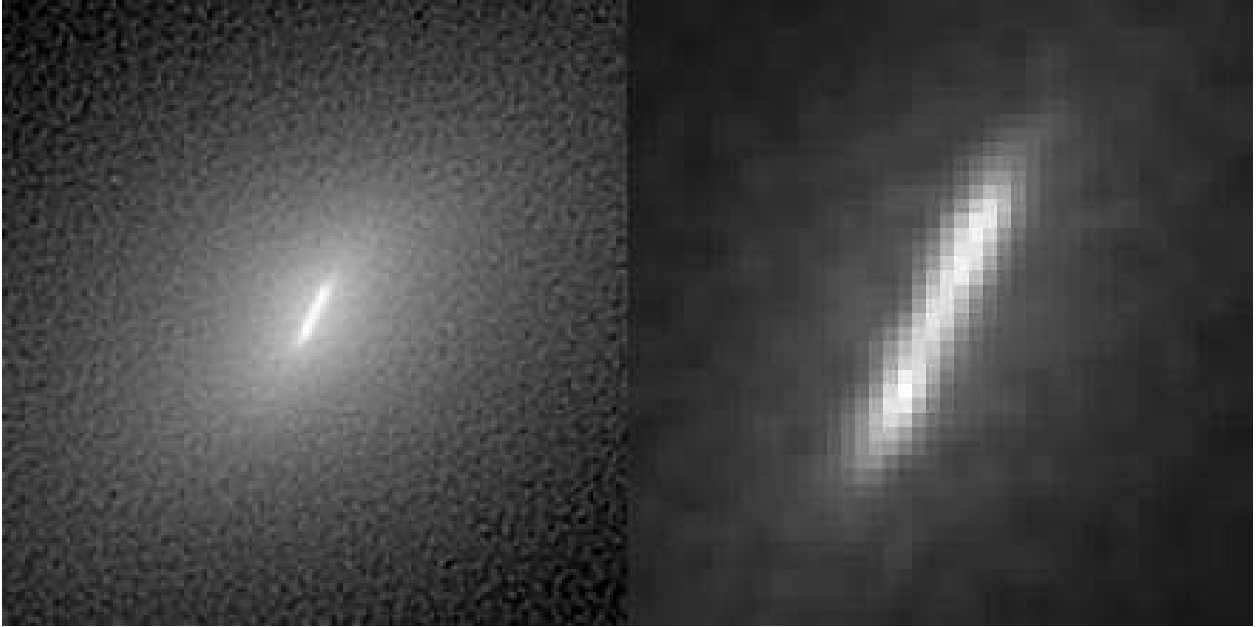


Fig. 1.— The F555W image of NGC 3706. The panel on the left shows the central $5'' \times 5''$ of the WFPC2 F555W image of NGC 3706. The galaxy was centered on the PC1 chip. The image is double-sampled, deconvolved, and displayed with a logarithmic stretch. The right panel is magnified by a factor of 5 to show the ring itself; the stretch is linear in this image. North is at 219.0° measured counterclockwise from the vertical axis.

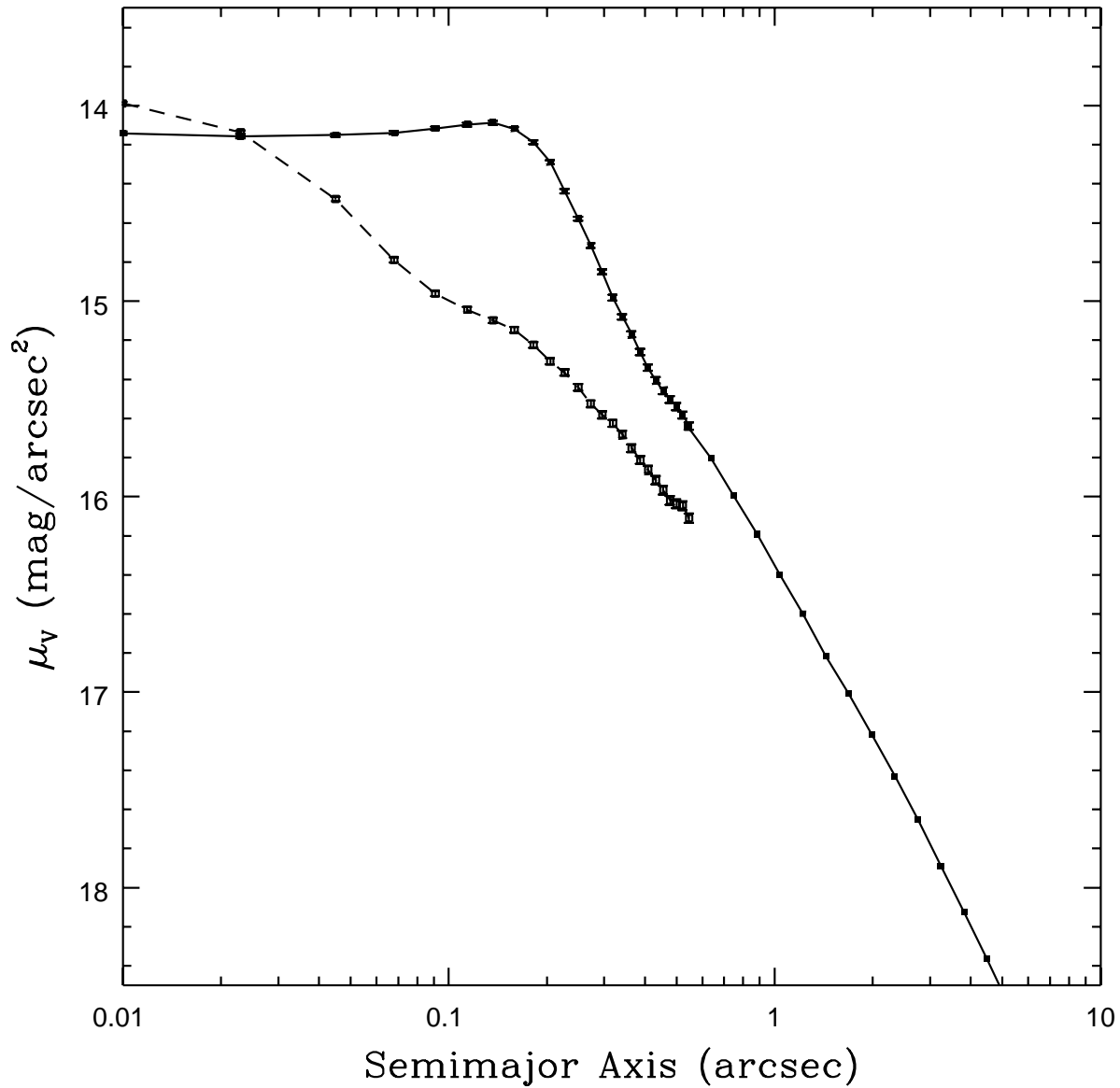


Fig. 2.— Surface brightness profiles for NGC 3706. The solid line is the major axis brightness profile. For $r < 0''.5$ the profile is measured from a cut ($0''.09$ in width) along the disk, with the opposite sides of the nucleus averaged. At larger radii, standard isophote fitting is used (connected dots). The dotted line is a cut perpendicular to the ring, again with both sides averaged.

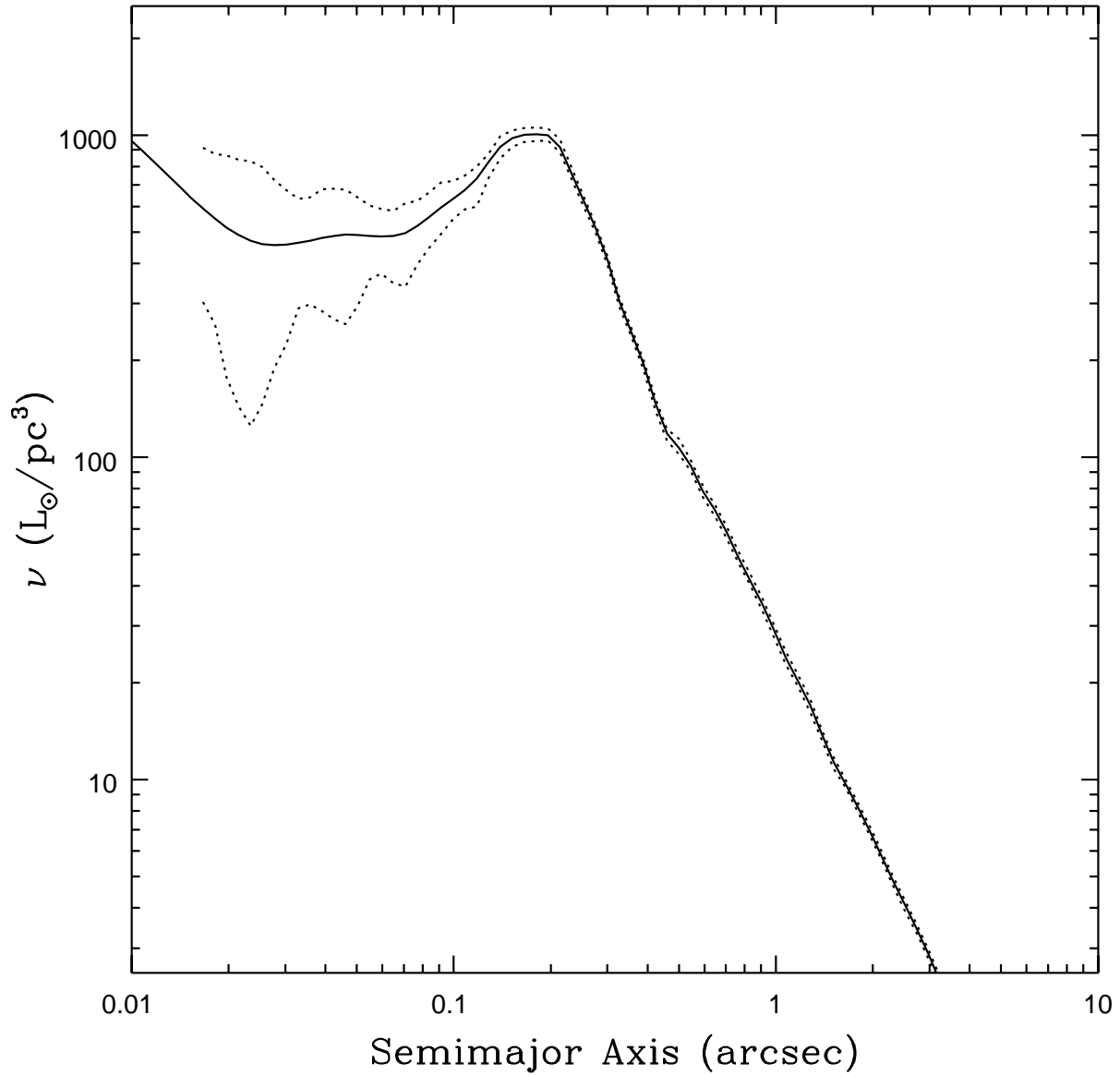


Fig. 3.— V-band luminosity density profile for the major axis of NGC 3706. Dashed lines give the $\pm 1\sigma$ error envelopes. The profile has been corrected for foreground extinction.

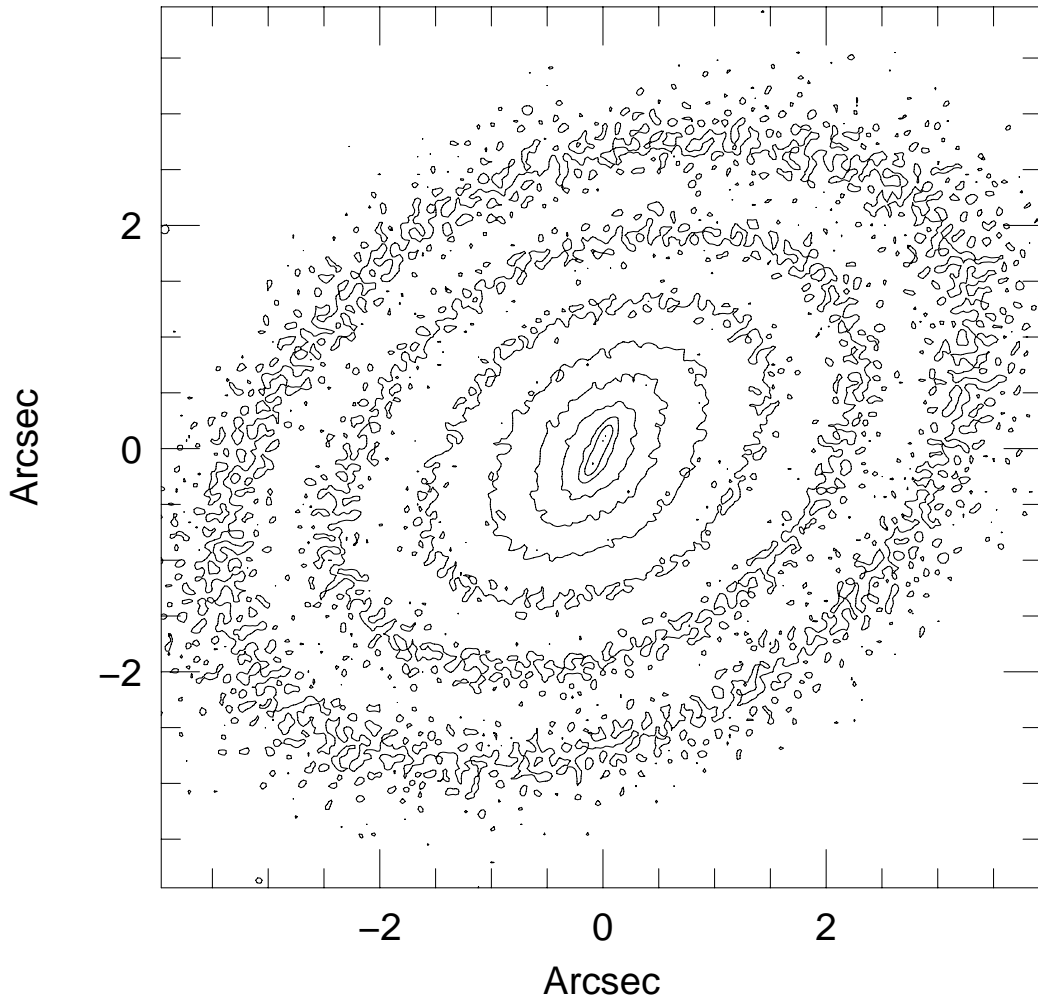


Fig. 4.— A contour map of NGC 3706 in the deconvolved F555W image. Contours are spaced by 0.5 mag in surface brightness; the outermost contour corresponds to $\mu_V = 18.0 \text{ mag arcsec}^{-2}$. North is at 219.0° measured counterclockwise from the vertical axis.

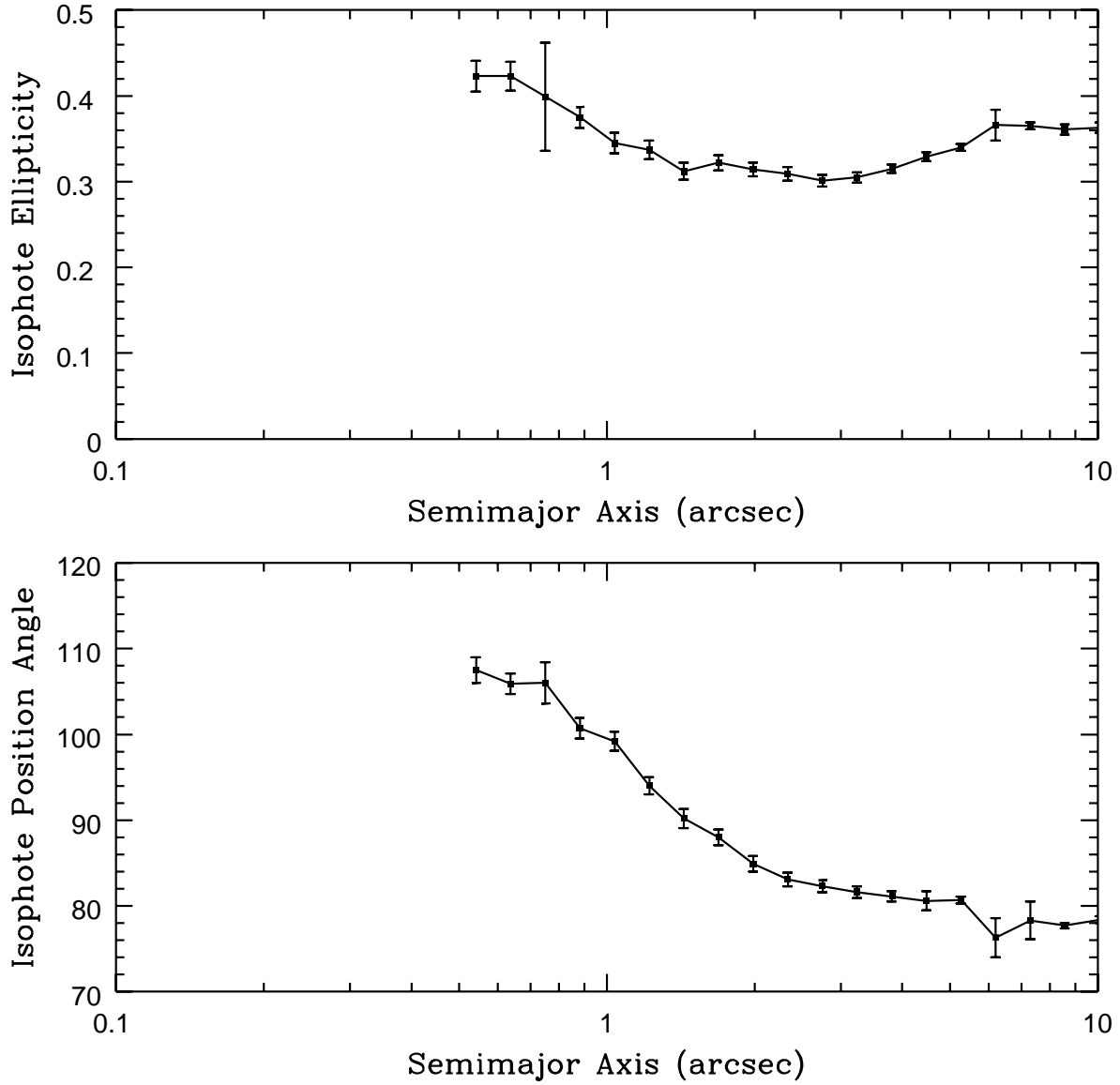


Fig. 5.— Isophote ellipticity and position angle profiles for NGC 3706. No points are shown for isophotes with semimajor axes $< 0''.5$, as these isophotes are poorly fitted by ellipses.

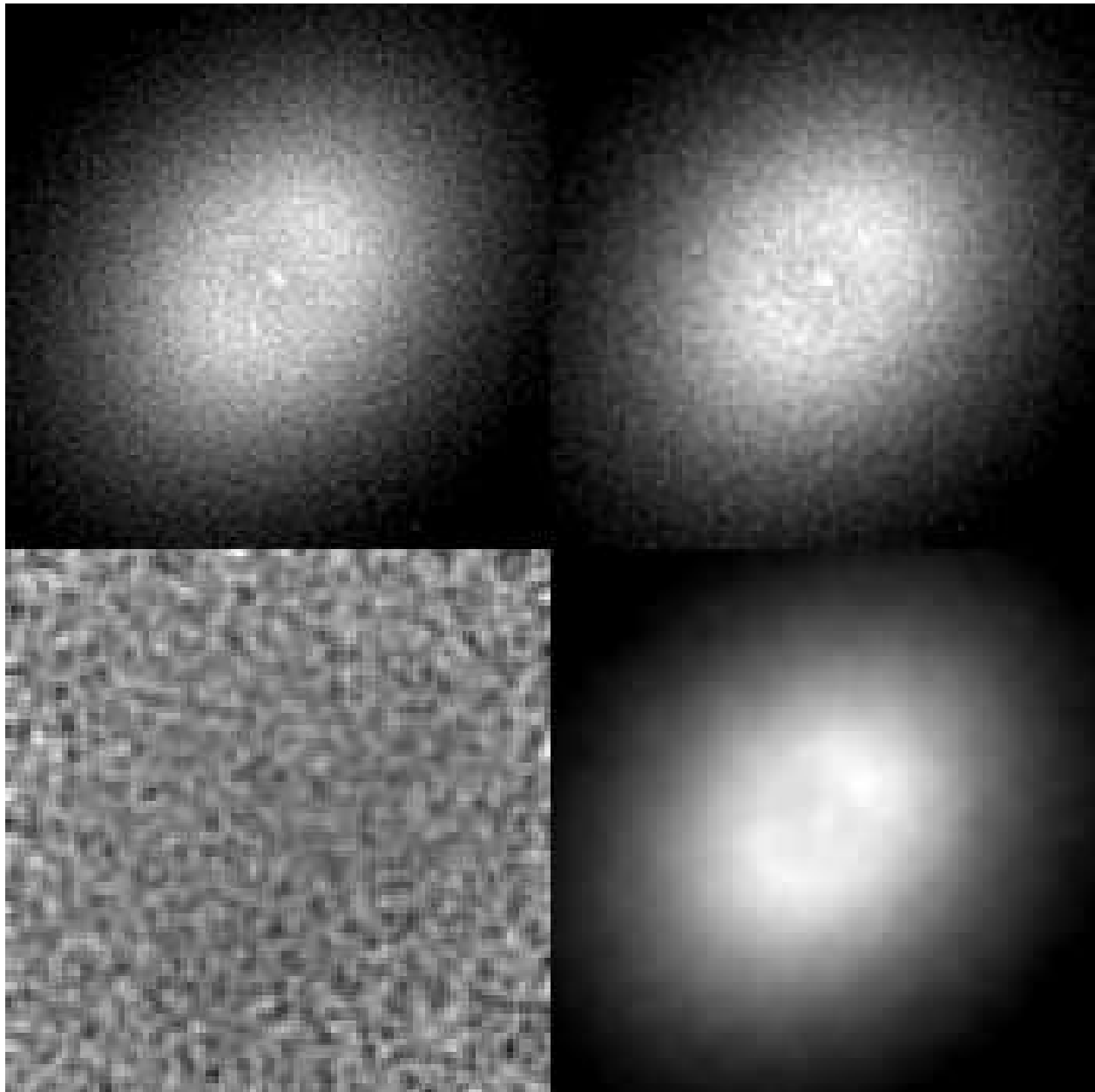


Fig. 6.— Images of NGC 4406 are shown in three different filters. The upper left and upper right panels are the deconvolved WFPC2 F555W and F814W images. The lower right panel is the deconvolved NIC2 F160W image resampled and rotated to match the WFPC2 images. The area of the panels is $4'' \times 4''$. An arbitrary linear stretch (the same in all three panels) has been used to enhance contrast in the core. The lower left panel is a slightly smoothed F555W/F814W ratio image; the full range of its gray scale is $\pm 10\%$. North is 8.9° measured counterclockwise from the vertical axis. The nuclear point-source is most evident in the V -band image.

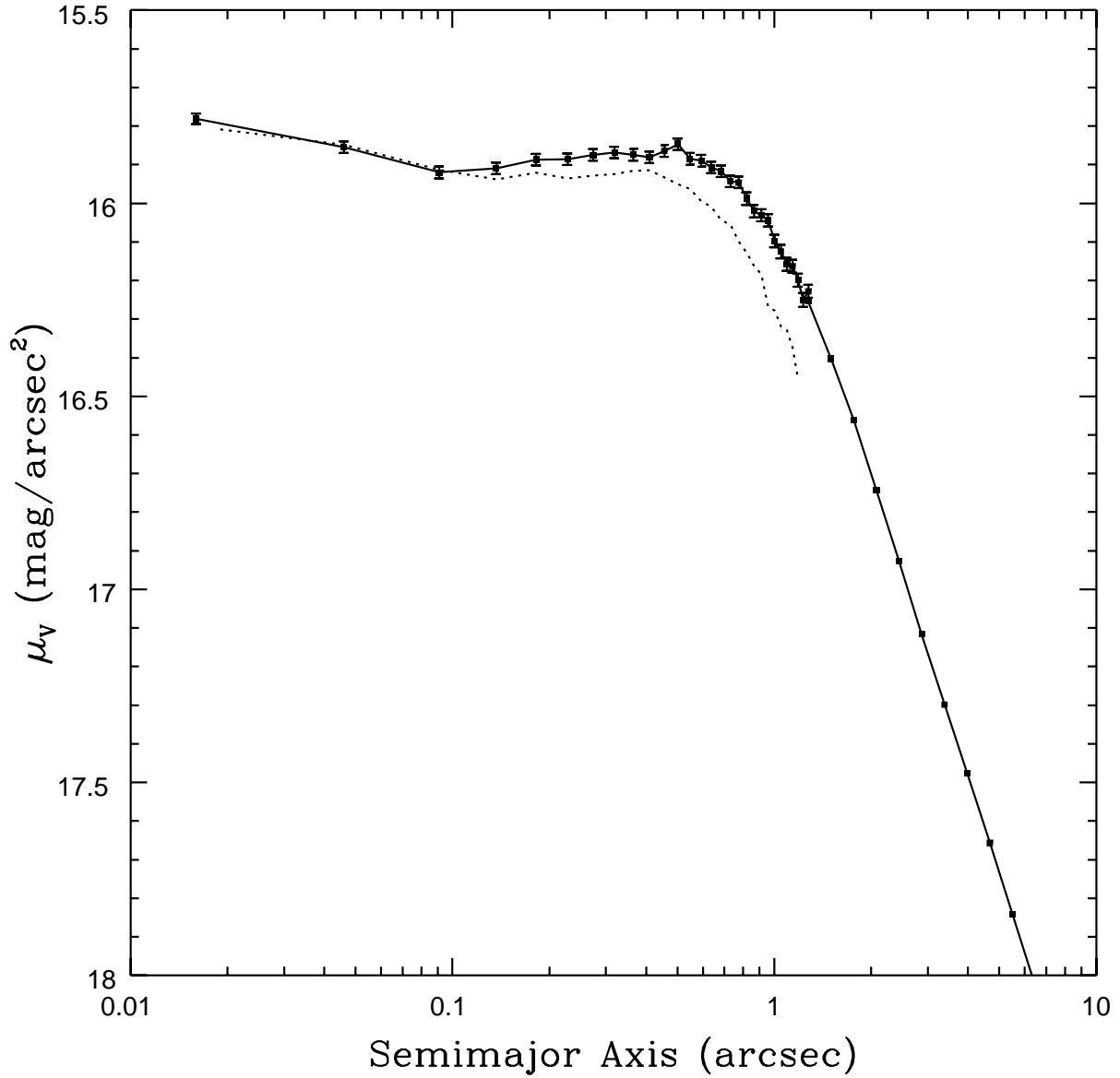


Fig. 7.— Major axis (solid) and minor axis (dotted) deconvolved F555W brightness profile for NGC 4406. The profile at $r > 1''.2$ was measured by isophote fitting (connected dots). At smaller radii the profile for each axis was measured from a cut along the axis (of width $0''.14$), with the opposite sides across the nucleus averaged.

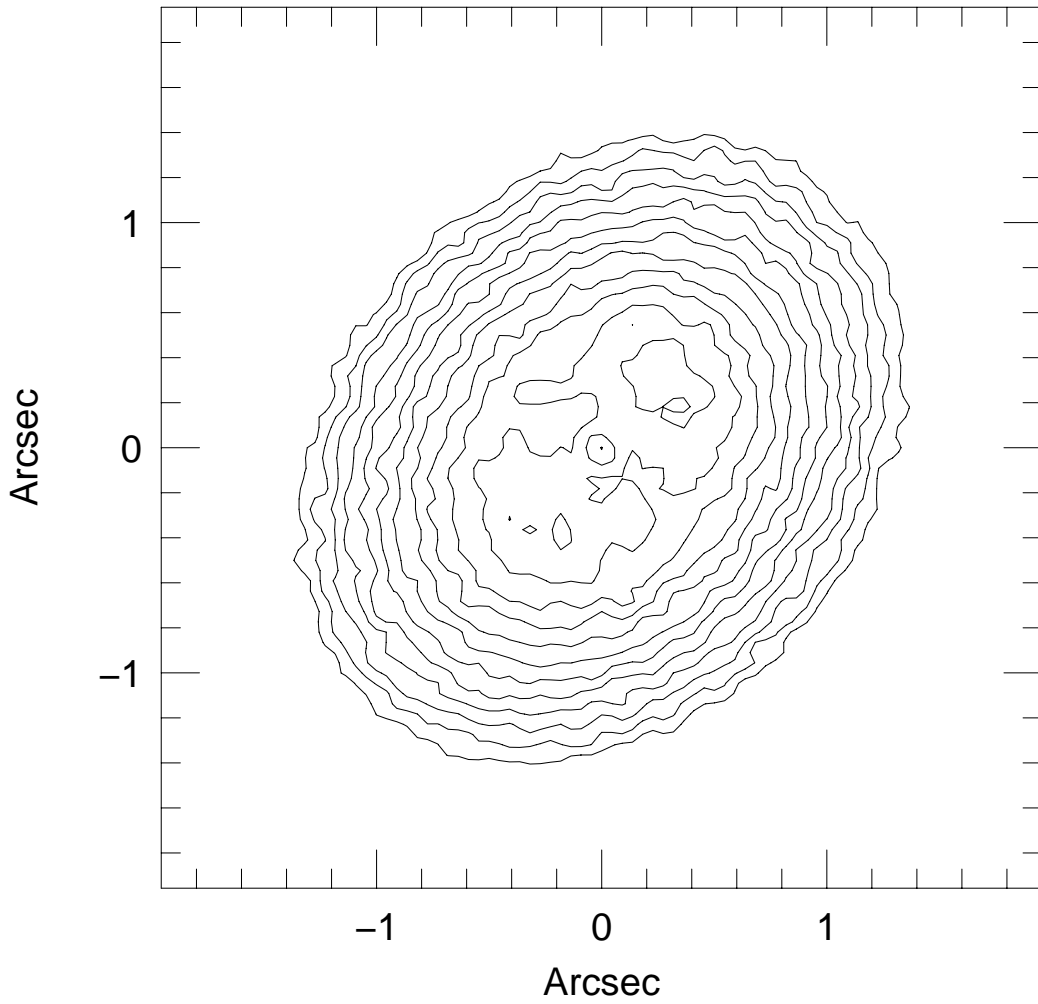


Fig. 8.— A contour map of NGC 4406 in the deconvolved F555W image. Contours are spaced by 0.05 mag in surface brightness; the outermost contour corresponds to $\mu_V = 16.42 \text{ mag arcsec}^{-2}$. North is 8.9° measured counterclockwise from the vertical axis.

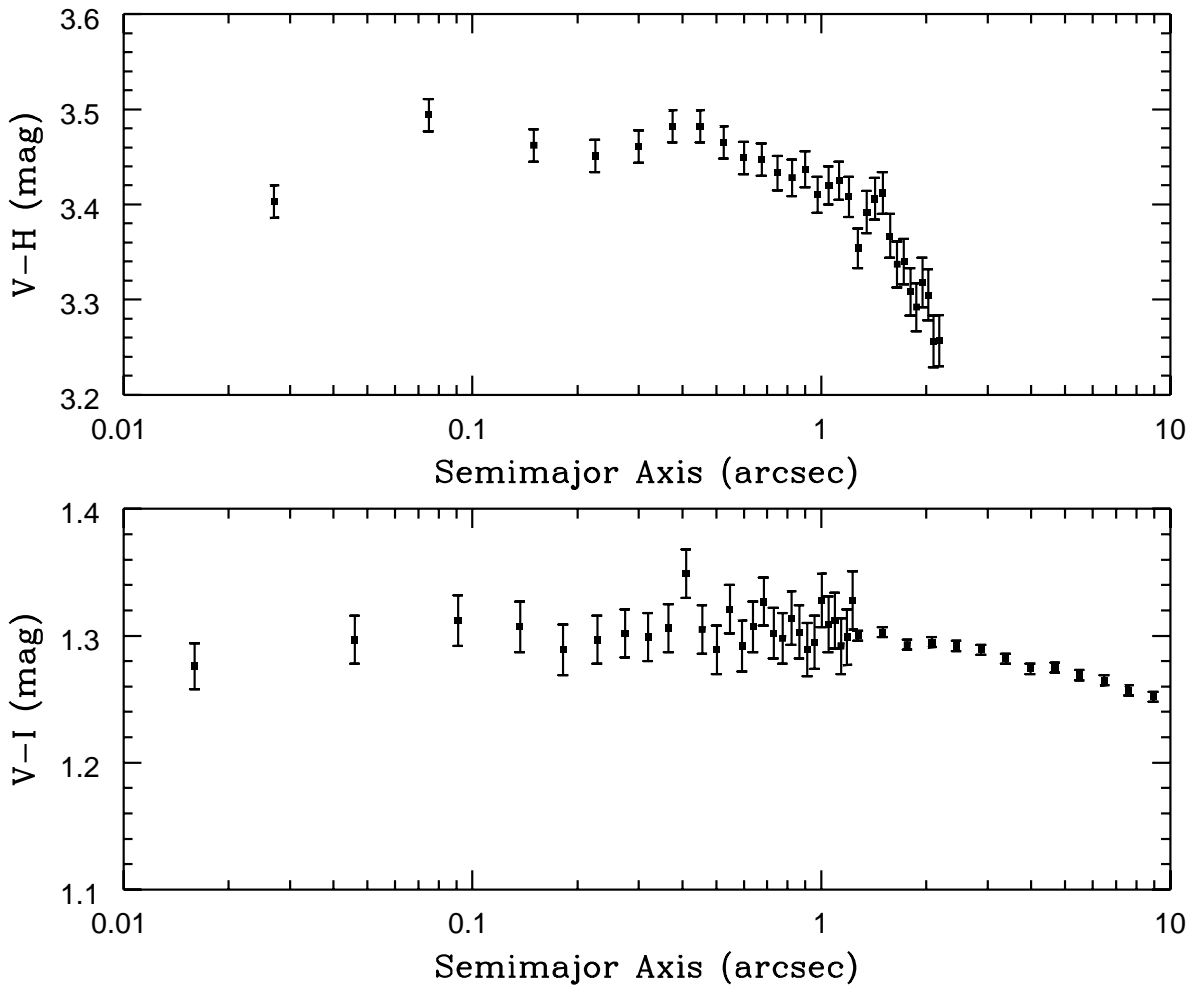


Fig. 9.— Major axis $V - H$ and $V - I$ color profiles of NGC 4406.

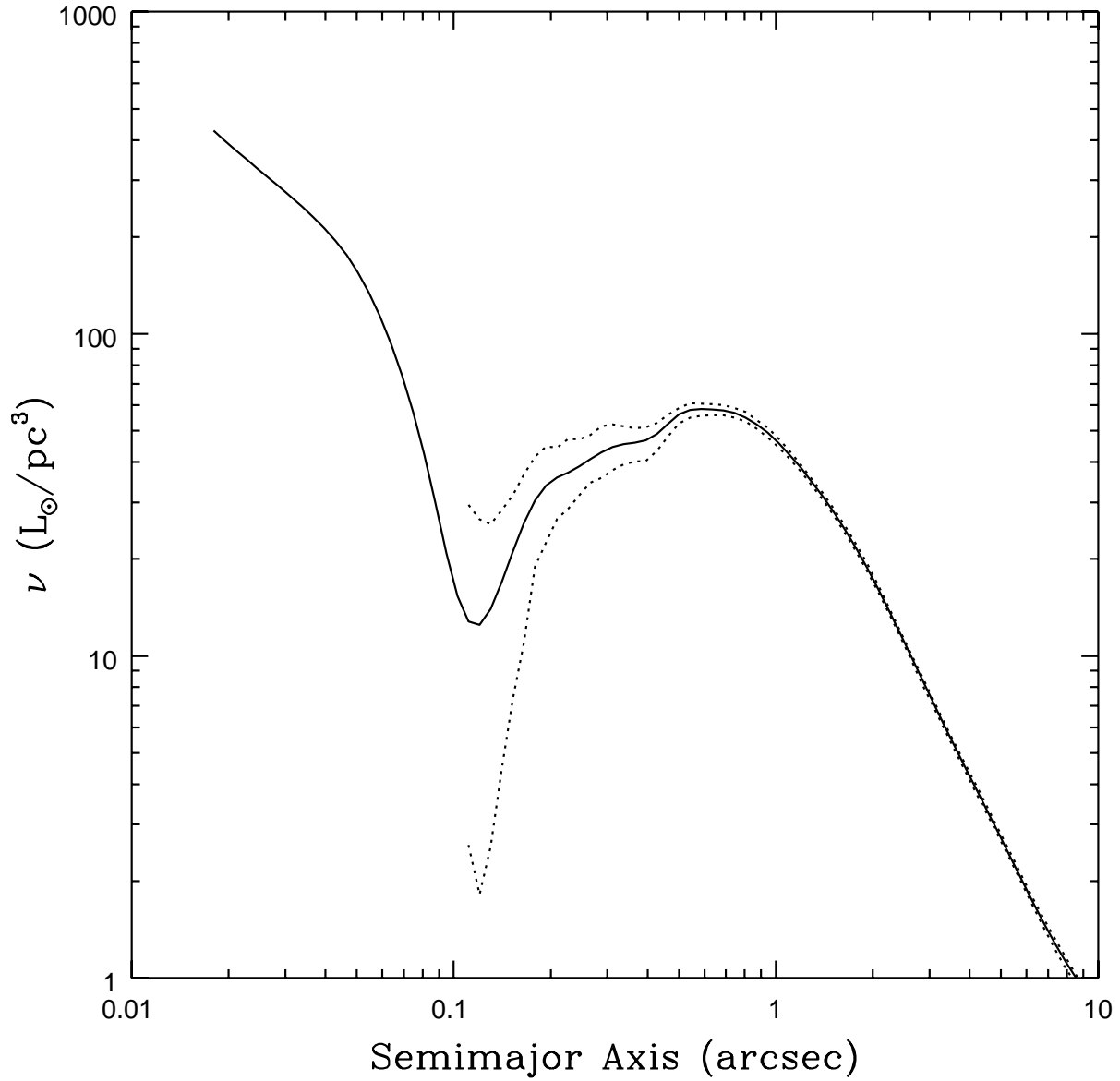


Fig. 10.— V -band luminosity density profile for the major axis of NGC 4406. Dashed lines give the $\pm 1\sigma$ error envelopes. The profile has been corrected for foreground extinction.

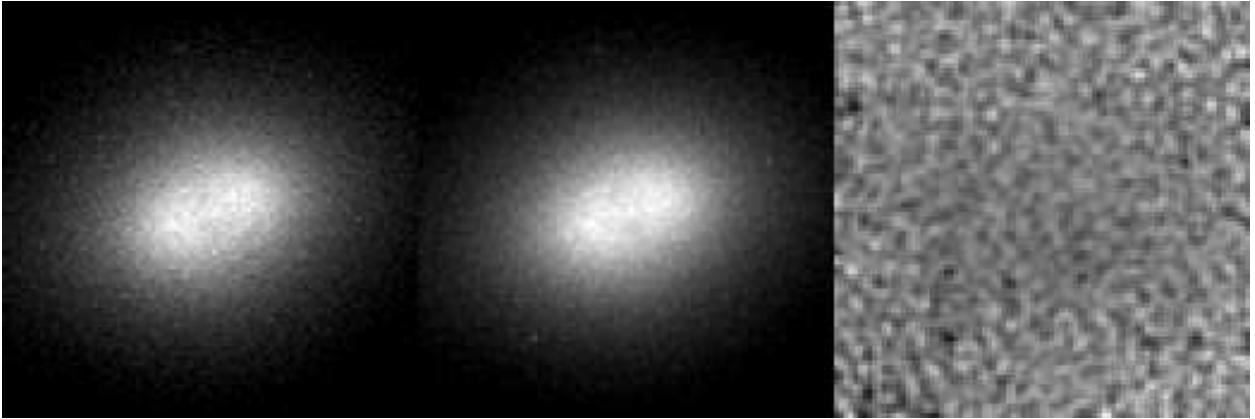


Fig. 11.— Images of the NGC 6876 core are shown in two filters. The left and middle panels are the deconvolved WFPC2 F555W and F814W images. The area of the panels is $4'' \times 4''$. An arbitrary linear stretch has been used to enhance contrast in the core. The right panel is a slightly smoothed F555W/F814W ratio image; the full range of its gray scale is $\pm 10\%$. North is 24.1° measured counterclockwise from the vertical axis.

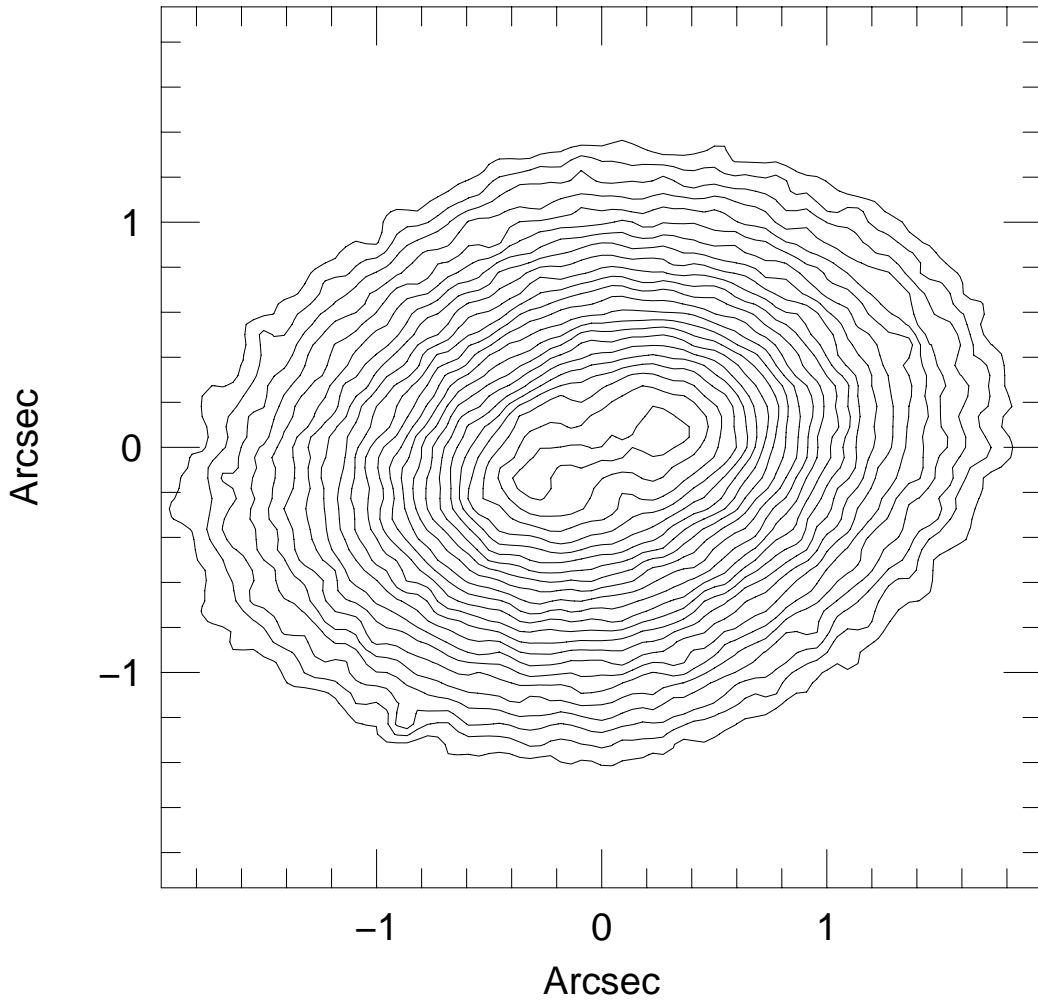


Fig. 12.— A contour map of NGC 6876 in the deconvolved F814W image. Contours are spaced by 0.05 mag in surface brightness; the outermost contour corresponds to $\mu_I = 16.71 \text{ mag arcsec}^{-2}$. North is 24.1° measured counterclockwise from the vertical axis.

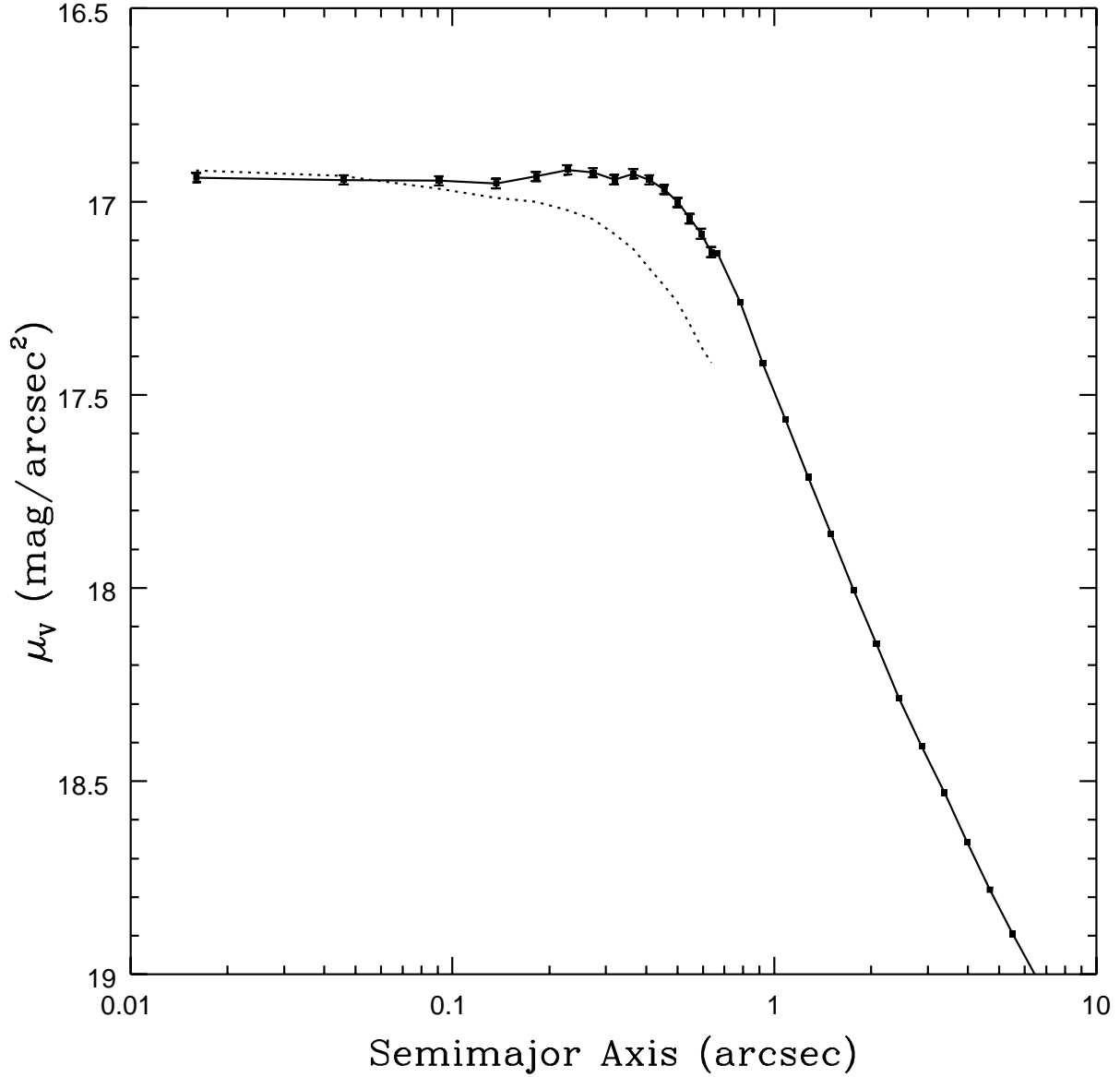


Fig. 13.— Major axis (solid) and minor axis (dotted) deconvolved F555W brightness profile for NGC 6876. The profile at $r > 0''.7$ was measured by isophote fitting (connected dots). At smaller radii the profile for each axis was measured from a cut along the axis (of width $0''.14$), with the opposite sides across the nucleus averaged.

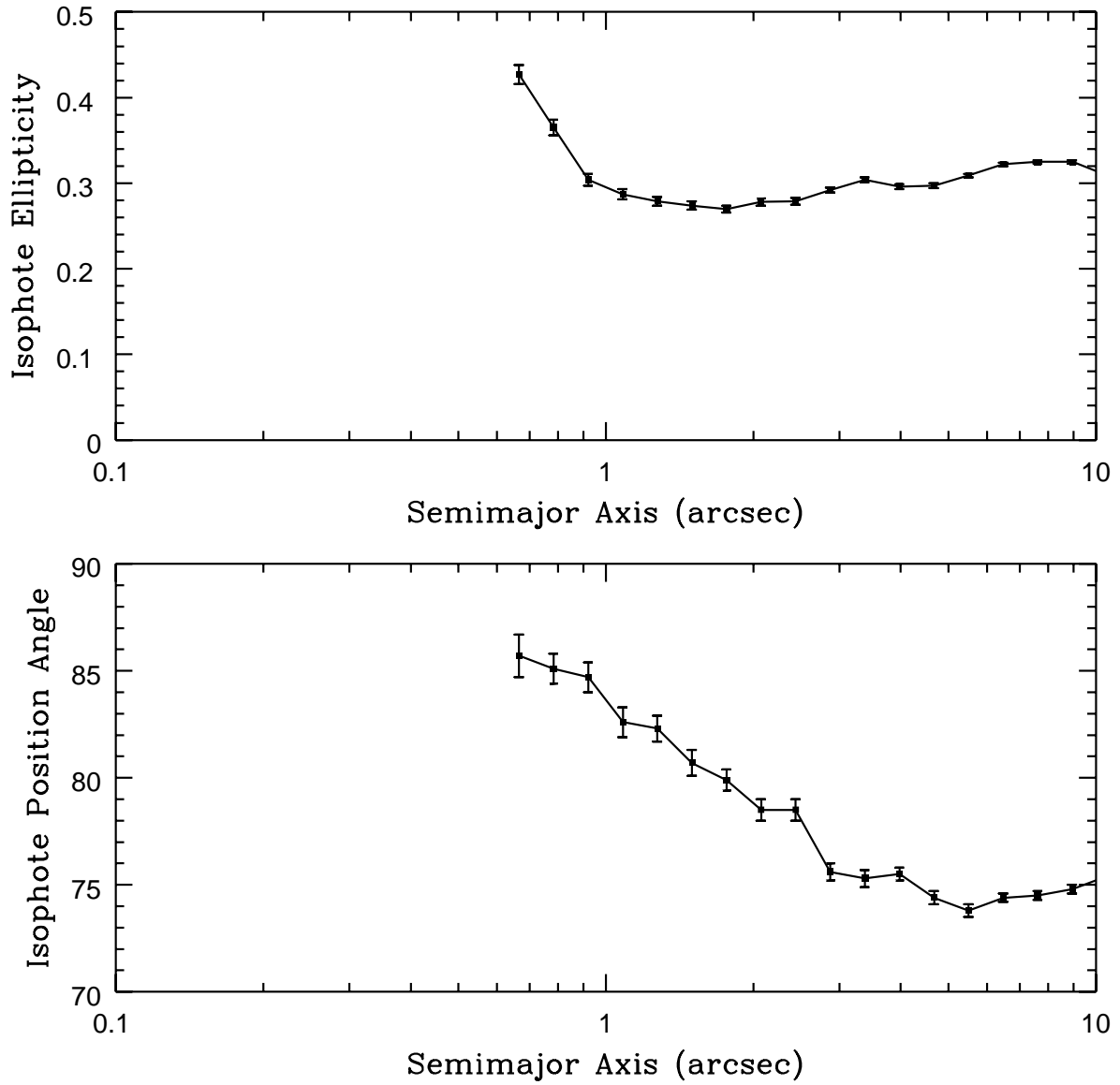


Fig. 14.— Isophote ellipticity and position angle profiles for NGC 6876. No points are shown for isophotes with semimajor axes $< 0''.6$, as these isophotes are poorly fitted by ellipses.

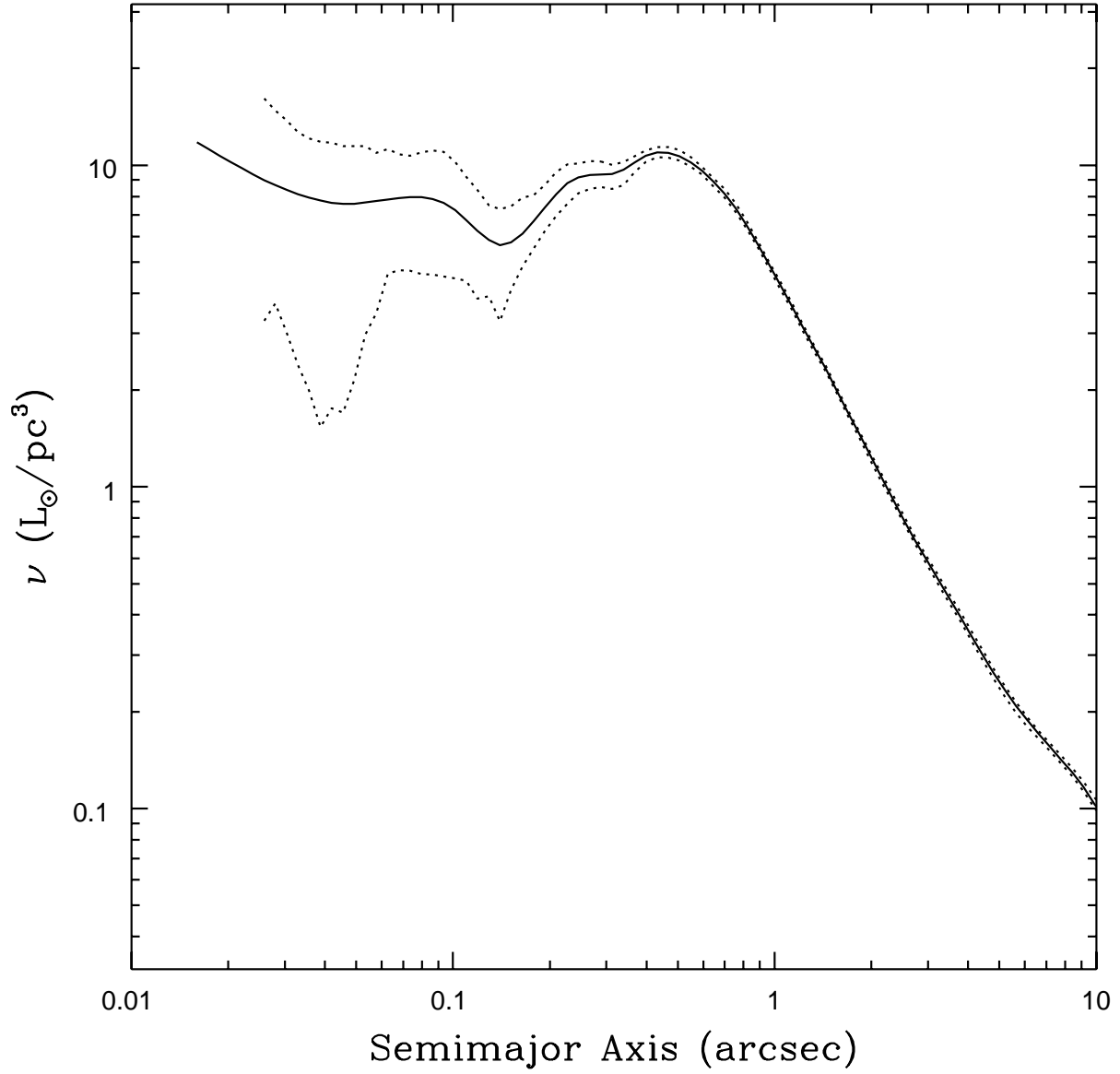


Fig. 15.— V -band luminosity density profiles for the major axis of NGC 6876. Dashed lines give the $\pm 1\sigma$ error envelopes. The profile has been corrected for extinction.



Fig. 16.— Three BCG candidates with centrally depressed stellar density profiles. Left to right, the galaxies are the BCG in A260, A347, and A3574. Each panel is a $4'' \times 4''$ subset of the deconvolved F814W PC snapshot image. The intensity stretch is arbitrary. North is 98.6° measured clockwise from the vertical axis for A260, 175.1° measured counterclockwise from the vertical axis for A347, and 42.4° measured clockwise from the vertical axis for A3574. A faint point-source is visible in the A3574 core.

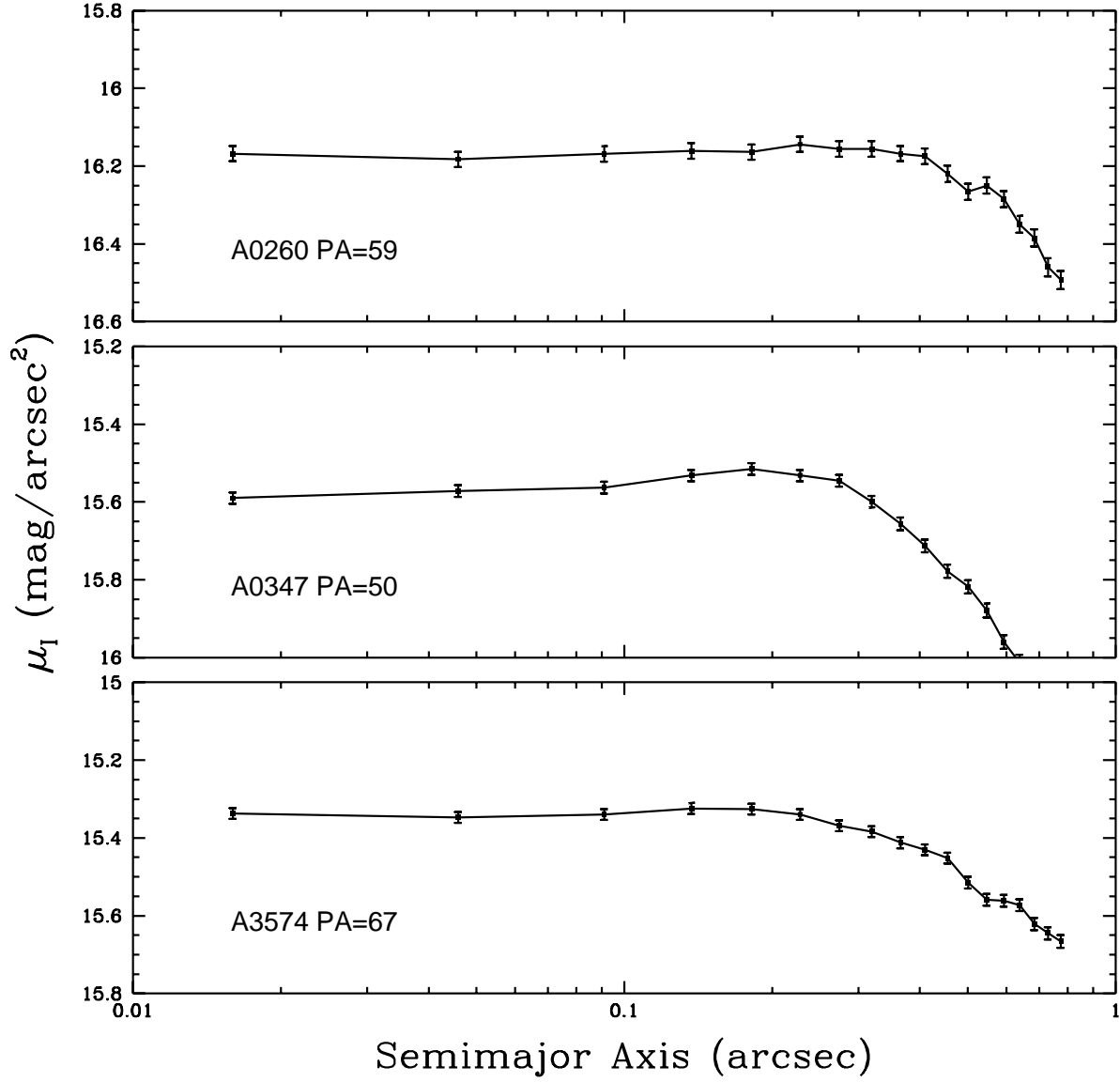


Fig. 17.— Surface brightness profiles are shown for the three BCG candidates with centrally depressed stellar density profiles. The profiles were measured from cuts along the major axis of width $0''.23$, with the opposite sides averaged. The position angles of the cuts are noted in each panel.